Published in final edited form as:
Semin Nucl Med. 2014 May ; 44(3): 172–178. doi:10.1053/j.semnuclmed.2014.03.007.

Dosimetry for Radiopharmaceutical Therapy

George Sgouros and **Robert F. Hobbs**
Johns Hopkins University, Baltimore, MD

Abstract

Radiopharmaceutical therapy (RPT) involves the use of radionuclides that are either conjugated to tumor-targeting agents (eg, nanoscale constructs, antibodies, peptides, and small molecules) or concentrated in tissue through natural physiological mechanisms that occur predominantly in neoplastic or otherwise targeted cells (eg, Graves disease). The ability to collect pharmacokinetic data by imaging and use this to perform dosimetry calculations for treatment planning distinguishes RPT from other systemic treatment modalities. Treatment planning has not been widely adopted, in part, because early attempts to relate dosimetry to outcome were not successful. This was partially because a dosimetry methodology appropriate to risk evaluation rather than efficacy and toxicity was being applied to RPT. The weakest links in both diagnostic and therapeutic dosimetry are the accuracy of the input and the reliability of the radiobiological models used to convert dosimetric data to the relevant biologic end points. Dosimetry for RPT places a greater demand on both of these weak links. To date, most dosimetric studies have been retrospective, with a focus on tumor dose-response correlations rather than prospective treatment planning. In this regard, transarterial radioembolization also known as intra-arterial radiation therapy, which uses radiolabeled (^{90}Y) microspheres of glass or resin to treat lesions in the liver holds much promise for more widespread dosimetric treatment planning. The recent interest in RPT with alpha-particle emitters has highlighted the need to adopt a dosimetry methodology that specifically accounts for the unique aspects of alpha particles. The short range of alpha-particle emitters means that in cases in which the distribution of activity is localized to specific functional components or cell types of an organ, the absorbed dose will be equally localized and dosimetric calculations on the scale of organs or even voxels (~5 mm) are no longer sufficient. This limitation may be overcome by using preclinical models to implement macromodeling to micromodeling. In contrast to chemotherapy, RPT offers the possibility of evaluating radiopharmaceutical distributions, calculating tumor and normal tissue absorbed doses, and devising a treatment plan that is optimal for a specific patient or specific group of patients.

Introduction

Radiopharmaceutical therapy (RPT) involves the use of radionuclides that are either conjugated to tumor-targeting agents (eg, nanoscale constructs, antibodies, peptides, and small molecules) or concentrated in tissue through natural physiological mechanisms that occur predominantly in neoplastic cells. In the latter category, radioiodine therapy of thyroid

Address reprint requests to George Sgouros, Johns Hopkins University, 4M61 CRB II, 1550 Orleans St, Baltimore, MD 21231. gsgouros@jhmi.edu.

cancer is the prototypical and most widely implemented RPT. In the category of radionuclide-ligand conjugates, antibody and peptide conjugates have been studied extensively.[1–4] The efficacy of RPT relies on the ability to delivery cytotoxic radiation to tumor cells without causing prohibitive normal tissue toxicity. After some 30 years of preclinical and clinical research, a number of recent developments suggest that RPT is poised to emerge as an important and widely recognized therapeutic modality. These developments include the substantial investment in antibodies by the pharmaceutical industry and the compelling rationale to build upon this already existing and widely tested platform. In addition, the growing recognition that the signaling pathways responsible for tumor cell survival and proliferation are less easily and durably inhibited than originally envisioned has also provided a rationale for identifying agents that are cytotoxic rather than inhibitory.[5–8] The success and recent Food and Drug Administration approval of the alpha-emitter ^{223}Ra ([^{223}Ra]$RaCl_2$, a calcium mimetic) for patients with prostate cancer with castration-resistant skeletal metastases[9] has also been an important impetus for reconsideration of RPT.

The recent interest in RPT with alpha-particle emitters has highlighted the need to adopt a dosimetry methodology that specifically accounts for the unique aspects of alpha particles.[10] Accordingly the review initially focuses on therapeutic dosimetry for low linear energy transfer (LET) emitters, beta particles, and photons. The dosimetry associated with alpha-particle emitters is considered separately. We begin with a discussion of dosimetry for low LET RPT.

Treatment Planning in RPT

The ability to collect pharmacokinetic (PK) data by imaging and use this to perform dosimetry calculations for treatment planning distinguishes RPT from other treatment modalities. The significance of this may be understood by comparison with chemotherapy dosing. Chemotherapy is administered on a per body weight or body surface area basis. Typically the dose used is based on a phase I dose escalation trial that determines the maximum tolerated dose (MTD). The MTD is defined by the response of a limited number of patients, typically 6 patients in a dose group. This MTD is then used to treat all other patients in phase II and subsequent trials. This approach does not account for differences in drug clearance, metabolism, or PK in different patients. The outcome of such an approach is that patients will either be underdosed (in RPT this is typically the case, as the MTD, when specified in terms of administered activity (AA) is conservatively chosen to avoid toxicity across most patients) or be overdosed and experience toxicity. In RPT, it is possible to collect PK and imaging data to calculate tumor and dose-limiting organ (DLO) absorbed dose (AD). AD is most closely related to tissue damage and normal organ toxicity. Thus AA can be adjusted to customize treatment for each patient to deliver the maximum possible AD to tumor without exceeding the AD to the DLO.

Matching the Dosimetry Methodology to the End Point

Such a scheme has not been widely adopted, in part, because early attempts to relate dosimetry to outcome were not successful. Dosimetry for RPT requires a fundamentally

different approach to that used for diagnosis. In diagnostic nuclear medicine, dosimetry is used primarily to evaluate the risk of cancer associated with the imaging procedure. In this context, the mean organ AD to a well-defined anatomical model is needed, as risk data are expressed in terms of mean organ AD to a model that is representative of the exposed (or imaged) population. In therapy, the relevant end points are organ toxicity and tumor control for the individual patient. This end point requires dosimetry that is substantially more detailed than the average over an organ or tumor volume. This information is required because the radiobiological models that yield toxicity and tumor control require dose-volume histograms and knowledge of the dose distribution to sensitive or dose-limiting portions of the tissue. These distinctions in input, dosimetry methodology, radiobiological modeling, and end points are summarized in Figure 1. The Table defines the quantities listed in the figure.

Dosimetry Methodology for Therapy End Points

As shown in Figure 1, a single value, the time-integrated activity (TIA) in each source organ is required as input into an AD calculation for diagnostic imaging wherein the end point is cancer and health detriment risk. The TIA is then used as an input into generic human models with representative anatomy. By contrast, evaluation of therapeutic end points, under most circumstances, uses the full voxelized information available Q11 from single photon emission CT (SPECT) and PET images, and also requires a registered CT scan, which provides the detailed patient-specific anatomical information, including the tumor. SPECT or PET provide the spatial activity information at different times following injection of the therapeutic radiopharmaceutical. The CT scan can be converted to a density map. The density map may be used to generate a tissue composition map by segmenting air, tissue, and bone according to standard density thresholds.[11,12] The density, composition, and activity maps are input to a Monte Carlo calculation (per time point) to obtain the patient-specific output indicated in Figure 1. If the differences in density and tissue composition are negligible, voxelized *S*-value and pointkernel methods may be used.[13,14] Techniques have also been developed to use voxelized *S*-value and point-kernel methods by making first-order adjustments to the AD map that account for a range of density variations.[15] The dosimetry output is converted to organ toxicity and tumor control using radiobiological models, which are largely based upon experience in external beam radiotherapy and brachytherapy.[16–19]

In the course of developing a new RPT, the best and most cost-effective time to implement patient-specific, 3-dimensional (3D) imaging–based methods is in the context of a phase I trial. The clinical end point for phase I trials is toxicity evaluation, other end points, including collection of imaging data for dosimetry and PK analysis, are also typically included to better understand the treatment. A simplified approach to incorporating treatment planning and 3D-based dosimetry methods in RPT is illustrated in Figure 2. In preclinical testing, the DLO and maximum tolerated AD are determined for a relevant model system. The AD to the dose-limiting or critical tissue is more closely related to potential toxicity than the AA. In such an approach, AA is increased in a relevant animal model until toxicity is reached. The organ responsible for dose-limiting toxicity is identified (eg, by necropsy or histopathology or both), and the AD to this organ at the toxic AA is calculated.

This information is used to design a phase I trial in which the escalation variable is the AD to the DLO. In such a trial the "dose" of activity administered is determined by a pretreatment imaging study that is used to obtain the PKs needed to calculate the AD to the DLO. At each AD level in the escalation scheme, the AA required to deliver the AD for each patient in the particular AD cohort is calculated. This means that patients in the same dose (AD) cohort may receive different AAs. In addition to providing the maximum tolerated AD, analysis of the data resulting from such a phase I study design will provide valuable information for future trials, especially in combination therapy investigations. In particular, if analysis of these data suggests that the advantage of treatment planning–based RPT is minimal for the given RPT and patient population, then treatment based on AA may be adequate as the AD delivered to the DLO is not highly dependent on individual patient's anatomy or PKs.

Limitations and Uncertainties

The weakest links in both diagnostic and therapeutic dosimetry are the accuracy of the input and the reliability of the radiobiological models used to convert dosimetric data to the relevant biologic end points. Dosimetry for RPT places a greater demand on both of these weak links. Typically, the activity distribution input is at the voxel or multi-voxel level. Reliable results at this level require correction for partial volume and spill-in or spill-out effects as well as corrections for scatter and attenuation.[20–24] Experience with the software package, 3D-radiobiological dosimetry, has shown that voxelized AD, averaged over an organ volume compares very well with the average absorbed-dose-to-an-organ volume.[25,26] The former is obtained by calculating the ADto each voxel and then taking the average of all AD values in a collection of voxels that define an organ volume. The latter is obtained directly from a Monte Carlo calculation in which the energy deposited to the organ volume is tallied and then divided by the mass of the volume (as obtained from the density map).

Radiobiological models in radiopharmaceutical dosimetry present a more fundamental problem particularly because their use requires parameter values that are almost always approximations of their true value. The radiation and tissue-weighting factors for cancer risk end points represent consensus values obtained by Committee review of relevant epidemiologic and biological data.[27–29] In therapy, although there is a consensus of appropriate values for different organ and tumor types, there is no standardization of values analogous to that in the radiation protection realm. In part, this is because the radiobiological parameter values relevant to therapy depend on a host of complex factors. In normal tissue, these factors include organ architecture, treatment history of the patient, and the general metabolic and physiological state of the organ. Radiobiological parameter values in tumors are affected by tumor type and by a number of tumor biology-specific factors that include the hypoxic and metabolic or proliferative fraction of the tumor. Depending upon the scale of the dosimetry calculation, the radiobiological parameters will vary across the normal tissue or tumor volume. The radiosensitivity of different normal tissue components is already known to be spatially dependent.[30–32] This is particularly important for RPT wherein the agent may concentrate within a subset of the cells making up a particular organ. Currently, dosimetry calculations of the type shown in Figure 1 for therapy assume a single set of radiobiological parameter values for all cells making up a tumor or normal organ.

From a practical standpoint, implementation of AD-based treatment planning requires the ability to acquire the necessary images from pretherapeutic administrations and perform the dosimetric calculations, including the Monte Carlo simulations, in a clinical time frame.[33] To date, most dosimetric studies have been retrospective, with a focus on tumor dose-response correlations rather than prospective treatment planning, although a number of schemata for such treatment planning have been proposed.[34–40] In this regard, transarterial radioembolization (TARE) also known as intra-arterial radiation therapy, which uses radiolabeled (^{90}Y) microspheres of glass or resin to treat lesions in the liver holds much promise for more widespread dosimetric treatment planning.[41–44] As the spheres stick (embolize) in the vasculature of the liver and tumors, there is no relocalization of activity typical of RPT and a single image suffices to provide the requisite dosimetric guidance. The growing interest in TARE dosimetry has also been fueled in large part by the recently discovered ability to image ^{90}Y with either (1) PET owing to a low branching ratio (32 ppm) of internal conversion positron production,[45],[46] or (2) SPECT imaging of the bremsstrahlung photons.[47] The caveat for TARE treatment planning, however, is the difference in the nature of the pretherapeutic radiopharmaceutical, ^{99m}Tc-labeled macroalbumin aggregate, which could potentially have a different biodistribution than the therapeutic microspheres. The predictive ability of the pretherapeutic macroalbumin aggregate remains controversial.[48–50]

Dosimetry for Alpha-Particle Emitting Radiopharmaceuticals

This topic was recently extensively reviewed.[10,51,52] In this section, we present specific examples that illustrate the dosimetry approach required for alpha-particle emitter RPT.

Alpha-particle emitters are attractive alternatives to traditional RPT or chemotherapy as a systemic cancer treatment because of their high-energy deposition (LET) over a relatively short range (50–100 μm). The number of hits for cell kill is orders of magnitude fewer than for traditional RPT (3–4 for alphas vs thousands for betas). This is due to the higher LET, but also because the biological effect of alpha radiation differs from other, previously used types of radiation such as beta-particle emitters. AD from alpha emitters is approximately 5 times more potent than AD from beta emitters or external beam radiation[10]; this is termed the relative biological effectiveness (RBE). Although a value of 5 is nominally used, the RBE can change substantially if modulators of DNA repair pathways are used.[53]

High LET radiation is also more damaging to normal organ cells; moreover, the short range of alpha-particle emitters means that in cases in which the distribution of activity is localized to specific functional components or cell types of an organ, the AD will be equally localized and dosimetric calculations on the scale of organs or even voxels (~5 mm) are no longer sufficient. Currently, no modalities are available to image activity at that scale clinically; therefore, models are being developed to supplement the information provided by the SPECT or PET images. The principle is to measure microdistribution of activity over time specific to an organ and radiopharmaceutical using preclinical ex vivo data imaged with an alpha-camera.[54] Based on these measurements, an apportionment of TIA to substructures can be made using traditional macroscopic imaging (macromodeling to micromodeling). TIA is then converted to AD apportioned to the different organ substructures based on

Monte Carlo simulations of radioisotope decay using idealized anatomical models of the organ substructures. This technique is highly analogous Q15 to the traditional Medical Internal Radiation Dose absorbed fraction methodology[55–57] as well as the kidney subunit model (with delineation of cortex, medulla and renal pelvis) designed with peptide receptor radiation therapy in mind.[31,32] Several examples of this alpha-particle dosimetry modeling paradigm have already been published,[58–60] 2 of which we present here briefly.

The model for the kidney was inspired by preclinical results using ^{225}Ac-labeled antibody to treat metastatic breast cancer to the lungs.[61] The treatment showed efficacy, but renal toxicity was observed at average ADs (~2 Gy) well below those consistent with toxicity, even taking into account the RBE. A nephron-based model, with compartments for the glomeruli, believed to be the more radiosensitive cells in the kidney, as well as a potential activity localization point, along with the proximal tubule cells and the distal tubule cells. *S*-values for the compartments and the different potential isotopes were calculated.[58]

A different scenario holds true for clinical results from the [^{223}Ra]$RaCl_2$ therapy of prostate cancer bone metastases. Traditional absorbed fraction dosimetry predicts a much higher level of hematotoxicity than experienced clinically[9]; which, although beneficial for the patients, impedes the possibility of any dosimetric-based treatment planning. Here, a simple trabecular marrow cavity model was proposed, wherein the fraction of marrow volume receiving a cytotoxic AD was calculated. The discrepancy between an absorbed fraction methodology and a method that specifically accounts for the dose distribution within the marrow cavity could then be explained because a substantial portion of the marrow cavity was not being irradiated.[59]

Other approaches for alpha-particle dosimetry, generally microdosimetric in nature, have been proposed and are being developed[62–67]; however, the advantage of the small-scale modeling approach is the ability to be applied to clinical imaging and dosimetry.

Future Directions

Several factors favor the adoption of AD-based treatment planning in the years to come: (1) the more widespread use of combined 3D imaging modalities, such as SPECT/CT, PET/CT (and PET/MRI), as well as the improved reconstruction techniques now available that together provide much more accurate and reliable quantitative data as input[68,69]; (2) the development of more 3D dosimetry packages, which are able to exploit such data[70–73]; and (3) the focus by the National Institutes of Health on the development of more personalized medicine.[74]

Additionally, the encouraging clinical and preclinical results from alpha-particle emitter RPT foreshadow a greater role to be played by alpha emitters in the fight against cancer, although the alpha-dosimetry models are still in their early stages and application of dosimetric treatment planning for alpha-particle emitter RPT is an important research area. In this context, the stochastic nature of alpha-emitter radiation, due to the short range and high potency at relatively low number of hits has not yet been well integrated into the dosimetry models and need to be better understood.

Finally, in the war on cancer, successful therapies often depend upon combination strategies involving different modalities. Development and use of dosimetric paradigms that will enable optimal integration of the different modalities will play a pivotal role in the success of combined RPT-RPT strategies,[36,75–77] as well as for combinations with other modalities.[35,40,53,78]

References

1. Witzig TE, Gordon LI, Cabanillas F, et al. Randomized controlled trial of yttrium-90-labeled ibritumomab tiuxetan radioimmunotherapy versus rituximab immunotherapy for patients with relapsed or refractory low-grade, follicular, or transformed B-cell non-Hodgkin's lymphoma. J Clin Oncol. 2002; 20(10):2453–2463. [PubMed: 12011122]
2. Press OW, Eary JF, Gooley T, et al. A phase I/II trial of iodine-131-tositumomab (anti-CD20), etoposide, cyclophosphamide, and autologous stem cell transplantation for relapsed B-cell lymphomas. Blood. 2000; 96(9):2934–2942. [PubMed: 11049969]
3. Kwekkeboom DJ, Mueller-Brand J, Paganelli G, et al. Overview of results of peptide receptor radionuclide therapy with 3 radiolabeled somatostatin analogs. J Nucl Med. 2005; 46(suppl 1):62S–66S. [PubMed: 15653653]
4. Bodei L, Pepe G, Paganelli G. Peptide receptor radionuclide therapy (PRRT) of neuroendocrine tumors with somatostatin analogues. Eur Rev Med Pharmacol Sci. 2010; 14(4):347–351. [PubMed: 20496546]
5. Downward J, Targeting RAF. Trials and tribulations. Nat Med. 2011; 17(3):286–288. [PubMed: 21383738]
6. Garrett JT, Arteaga CL. Resistance to HER2-directed antibodies and tyrosine kinase inhibitors: Mechanisms and clinical implications. Cancer Biol Ther. 2011; 11(9):793–800. [PubMed: 21307659]
7. Skorski T. Chronic myeloid leukemia cells refractory/resistant to tyrosine kinase inhibitors are genetically unstable and may cause relapse and malignant progression to the terminal disease state. Leuk Lymphoma. 2011; 52(suppl 1):23–29. [PubMed: 21299457]
8. Gorre ME, Mohammed M, Ellwood K, et al. Clinical resistance to STI-571 cancer therapy caused by BCR-ABL gene mutation or amplification. Science. 2001; 293(5531):876–880. [PubMed: 11423618]
9. Lewington, VJ.; Parker, C.; Hindorf, C., et al. Alpharadin: A novel, targeted approach for treatment of bone metastases from CRPC-calculated alpha-particle dosimetry compared to a favorable clinical safety profile. San Francisco, CA: ASCO Genitourinary Cancers Symposium; 2010.
10. Sgouros G, Roeske JC, McDevitt MR, et al. MIRD pamphlet no. 22 (abridged): Radiobiology and dosimetry of alpha-particle emitters for targeted radionuclide therapy. J Nucl Med. 2010; 51(2): 311–328. [PubMed: 20080889]
11. Prideaux AR, Song H, Hobbs RF, et al. Three-dimensional radiobiologic dosimetry: Application of radiobiologic modeling to patient-specific 3-dimensional imaging-based internal dosimetry. J Nucl Med. 2007; 48(6):1008–1016. [PubMed: 17504874]
12. Sgouros, G.; Kolbert, KS. The three-dimensional internal dosimetry software package, 3D-ID. In: Zaidi, H.; Sgouros, G., editors. Therapeutic Applications of Monte Carlo Calculations in Nuclear Medicine. Philadelphia, PA: Institute of Physics; 2002. p. 249-261.
13. Dieudonne A, Hobbs RF, Bolch WE, et al. Fine-resolution voxel S values for constructing absorbed dose distributions at variable voxel size. J Nucl Med. 2010; 51(10):1600–1607. [PubMed: 20847175]
14. BolchWE, Bouchet LG, Robertson JS, et al. MIRD pamphlet no, 17: The dosimetry of nonuniform activity distributions—Radionuclide S values at the voxel level. Medical Internal Radiation Dose Committee. J Nucl Med. 1999; 40(1):11S–36S. [PubMed: 9935083]
15. Dieudonne A, Hobbs RF, Lebtahi R, et al. Study of the impact of tissue density heterogeneities on 3-dimensional abdominal dosimetry: Comparison between dose kernel convolution and direct Monte Carlo methods. J Nucl Med. 2013; 54(2):236–243. [PubMed: 23249540]

16. Niemierko A. Reporting and analyzing dose distributions: A concept of equivalent uniform dose. Med Phys. 1997; 24(1):103–110. [PubMed: 9029544]
17. Kutcher GJ, Burman C, Brewster L, et al. Histogram reduction method for calculating complication probabilities for three-dimensional treatment planning evaluations. Int J Radiat Oncol Biol Phys. 1991; 21(1):137–146. [PubMed: 2032884]
18. Bentzen SM, Constine LS, Deasy JO, et al. Quantitative analyses of normal tissue effects in the clinic (QUANTEC): An introduction to the scientific issues. Int J Radiat Oncol Biol Phys. 2010; 76(suppl 3):S3–S9. [PubMed: 20171515]
19. Dale RG. The application of the linear-quadratic dose-effect equation to fractionated and protracted radiotherapy. Br J Radiol. 1985; 58(690):515–528. [PubMed: 4063711]
20. Kadrmas DJ, Frey EC, Karimi SS, et al. Fast implementations of reconstruction-based scatter compensation in fully 3D SPECT image reconstruction. Phys Med Biol. 1998; 43(4):857–873. [PubMed: 9572510]
21. He B, Du Y, Song X, et al. A Monte Carlo and physical phantom evaluation of quantitative In-111 SPECT. Phys Med Biol. 2005; 50(17):4169–4185. [PubMed: 16177538]
22. Hudson HM, Larkin RS. Accelerated image reconstruction using ordered subsets of projection data. IEEE Trans Med Imaging. 1994; 13(4):601–609. [PubMed: 18218538]
23. Jentzen W. Experimental investigation of factors affecting the absolute recovery coefficients in iodine-124 PET lesion imaging. Phys Med Biol. 2010; 55(8):2365–2398. [PubMed: 20360631]
24. Jentzen W, Weise R, Kupferschlager J, et al. Iodine-124 PET dosimetry in differentiated thyroid cancer: Recovery coefficient in 2Dand 3Dmodes for PET(/CT) systems. Eur J Nucl Med Mol Imaging. 2008; 35(3):611–623. [PubMed: 17929014]
25. Senthamizhchelvan S, Hobbs RF, Song H, et al. Tumor dosimetry and response for ^{153}Sm-ethylenediamine tetramethylene phosphonic acid therapy of high-risk osteosarcoma. J Nucl Med. 2012; 53(2):215–224. [PubMed: 22251554]
26. Hobbs RF, Jentzen W, Bockisch A, et al. Monte Carlo-based 3-dimensional dosimetry of salivary glands in radioiodine treatment of differentiated thyroid cancer estimated using ^{124}I PET. Q J Nucl Med Mol Imaging. 2013; 57(1):79–91. [PubMed: 23474639]
27. The 2007 recommendations of the International Commission on Radiological Protection. ICRP Publication 103. Ann ICRP. 2007; 37(2–4):1–332.
28. Ann ICRP. 2003. Relative biological effectiveness (RBE), quality factor (Q), and radiation weighting factor (W_R): ICRP Publication 92.
29. Health Risks From Exposure to Low Levels of Ionizing Radiation: BEIR VII Phase 2. The National Academies Press; 2006.
30. Barone R, Borson-Chazot FO, Valkerna R, et al. Patient-specific dosimetry in predicting renal toxicity with Y-90-DOTATOC: Relevance of kidney volume and dose rate in finding a dose-effect relationship. J Nucl Med. 2005; 46:99S–106S. [PubMed: 15653658]
31. Bouchet LG, Bolch WE, Blanco HP, et al. MIRD pamphlet no 19: Absorbed fractions and radionuclide S values for six age-dependent multiregion models of the kidney. J Nucl Med. 2003; 44(7):1113–1147. [PubMed: 12843230]
32. Wessels BW, Konijnenberg MW, Dale RG, et al. MIRD pamphlet no, 20: The effect of model assumptions on kidney dosimetry and response— Implications for radionuclide therapy. J Nucl Med. 2008; 49(11):1884–1899. [PubMed: 18927342]
33. Hobbs RF, Wahl RL, Lodge MA, et al. ^{124}I PET-based 3D-RD dosimetry for a pediatric thyroid cancer patient: Real-time treatment planning and methodologic comparison. J Nucl Med. 2009; 50(11):1844–1847. [PubMed: 19837771]
34. Baechler S, Hobbs RF, Boubaker A, et al. Three-dimensional radiobiological dosimetry of kidneys for treatment planning in peptide receptor radionuclide therapy. Med Phys. 2012; 39(10):6118–6128. [PubMed: 23039651]
35. Hobbs RF, McNutt T, Baechler S, et al. A treatment planning method for sequentially combining radiopharmaceutical therapy and external radiation therapy. Int J Radiat Oncol Biol Phys. 2011; 80(4):1256–1262. [PubMed: 20950958]

36. Hobbs RF, Wahl RL, Frey EC, et al. Radiobiologic optimization of combination radiopharmaceutical therapy applied to myeloablative treatment of non-Hodgkin lymphoma. J Nucl Med. 2013
37. Pacilio M, Betti M, Cicone F, et al. A theoretical dose-escalation study based on biological effective dose in radioimmunotherapy with (90)Y-ibritumomab tiuxetan (Zevalin). Eur J Nucl Med Mol Imaging. 2010; 37(5):862–873. [PubMed: 20069297]
38. Chiesa C, Botta F, Di Betta E, et al. Dosimetry in myeloablative (90)Y-labeled ibritumomab tiuxetan therapy: Possibility of increasing administered activity on the base of biological effective dose evaluation. Preliminary results. Cancer Biother Radiopharm. 2007; 22(1):113–120. [PubMed: 17627419]
39. Chiesa C, Castellani MR, Vellani C, et al. Individualized dosimetry in the management of metastatic differentiated thyroid cancer. Q J Nucl Med Mol Imaging. 2009; 53(5):546–561. [PubMed: 19910908]
40. Ferrari ME, Cremonesi M, Di Dia A, et al. 3D dosimetry in patients with early breast cancer undergoing intraoperative avidination for radionuclide therapy (IART) combined with external beam radiation therapy. Eur J Nucl Med Mol Imaging. 2012; 39(11):1702–1711. [PubMed: 22890802]
41. Dieudonne A, Garin E, Laffont S, et al. Clinical feasibility of fast 3-dimensional dosimetry of the liver for treatment planning of hepatocellular carcinoma with ^{90}Y-microspheres. J Nucl Med. 2011; 52(12):1930–1937. [PubMed: 22068894]
42. Cremonesi M, Ferrari M, Bartolomei M, et al. Radioembolisationwith ^{90}Y-microspheres: Dosimetric and radiobiological investigation formulti-cycle treatment. Eur J Nucl Med Mol Imaging. 2008; 35(11):2088–2096. [PubMed: 18618108]
43. Strigari L, Sciuto R, Rea S, et al. Efficacy and toxicity related to treatment of hepatocellular carcinoma with ^{90}Y-SIR spheres: Radiobiologic considerations. J Nucl Med. 2010; 51(9):1377–1385. [PubMed: 20720056]
44. Chiesa C, Maccauro M, Romito R, et al. Need, feasibility and convenience of dosimetric treatment planning in liver selective internal radiation therapy with (90)Y microspheres: The experience of the National Tumor Institute of Milan. Q J Nucl Med Mol Imaging. 2011; 55(2):168–197. [PubMed: 21386789]
45. Lhommel R, Goffette P, Van den Eynde M, et al. Yttrium-90 TOF PET scan demonstrates high-resolution biodistribution after liver SIRT. Eur J Nucl Med Mol Imaging. 2009; 36(10):1696. [PubMed: 19618182]
46. van Elmbt L, Vandenberghe S, Walrand S, et al. Comparison of yttrium-90 quantitative imaging by TOF and non-TOF PET in a phantom of liver selective internal radiotherapy. Phys Med Biol. 2011; 56(21):6759–6777. [PubMed: 21970976]
47. Rong X, Du Y, Ljungberg M, et al. Development and evaluation of an improved quantitative (90)Y bremsstrahlung SPECT method. Med Phys. 2012; 39(5):2346–2358. [PubMed: 22559605]
48. Garin E, Lenoir L, Rolland Y, et al. Dosimetry based on ^{99m}Tcmacroaggregated albumin SPECT/CT accurately predicts tumor response and survival in hepatocellular carcinoma patients treated with ^{90}Y-loaded glass microspheres: Preliminary results. J Nucl Med. 2012; 53(2):255–263. [PubMed: 22302962]
49. Wondergem M, Smits ML, Elschot M, et al. ^{99m}Tc-macroaggregated albumin poorly predicts the intrahepatic distribution of ^{90}Y resin microspheres in hepatic radioembolization. J NuclMed. 2013; 54(8):1294–1301.
50. Lam MG, Goris ML, Iagaru AH, et al. Prognostic utility of ^{90}Y radioembolization dosimetry based on fusion ^{99m}Tc-macroaggregated albumin-^{99m}Tc-sulfur colloid SPECT. J Nucl Med. 2013
51. Sgouros G, Hobbs RF, Song H. Modelling and dosimetry for alphaparticle therapy. Curr Radiopharm. 2011; 4(3):261–265. [PubMed: 22201712]
52. Brechbiel MW. Targeted alpha therapy: Past, present, future? Dalton Trans. 2007; 43:4918–4928. [PubMed: 17992276]
53. Song H, Hedayati M, Hobbs RF, et al. Targeting aberrant DNA double strand break repair in triple negative breast cancer with alpha particle emitter radiolabeled anti-EGFR antibody. Mol Cancer Ther. 2013

54. Back T, Jacobsson L. The alpha-camera: A quantitative digital autoradiography technique using a charge-coupled device for ex vivo highresolution bioimaging of alpha-particles. J Nucl Med. 2010; 51(10):1616–1623. [PubMed: 20847171]
55. Bolch WE, Eckerman KF, Sgouros G, et al. MIRD pamphlet no, 21: A generalized schema for radiopharmaceutical dosimetry—Standardization of nomenclature. J Nucl Med. 2009; 50(3):477–484. [PubMed: 19258258]
56. Siegel JA, Thomas SR, Stubbs JB, et al. MIRD pamphlet no, 16: Techniques for quantitative radiopharmaceutical biodistribution data acquisition and analysis for use in human radiation dose estimates. J Nucl Med. 1999; 40(2):37S–61S. [PubMed: 10025848]
57. Snyder, WS.; Ford, MR.; Warner, GG., et al. "S," Absorbed Dose per Unit Cumulated Activity for Selected Radionuclides and Organs. New York, NY: Society of Nuclear Medicine; 1975. MIRD Pamphlet No. 11.
58. Hobbs RF, Song H, Huso DL, et al. A nephron-based model of the kidneys for macro-to-micro alpha-particle dosimetry. Phys Med Biol. 2012; 57(13):4403–4424. [PubMed: 22705986]
59. Hobbs RF, Song H, Watchman CJ, et al. A bone marrow toxicity model for (223)Ra alpha-emitter radiopharmaceutical therapy. Phys Med Biol. 2012; 57(10):3207–3222. [PubMed: 22546715]
60. Larsson E, Meerkhan SA, Strand SE, et al. A small-scale anatomic model for testicular radiation dosimetry for radionuclides localized in the human testes. J Nucl Med. 2011; 53(1):72–81. [PubMed: 22080442]
61. Song H, Hobbs RF, Vajravelu R, et al. Radioimmunotherapy of breast cancer metastases with alpha-particle emitter ^{225}Ac: Comparing efficacy with ^{213}Bi and ^{90}Y. Cancer Res. 2009; 69(23): 8941–8948. [PubMed: 19920193]
62. Akabani G, Kennel SJ, Zalutsky MR. Microdosimetric analysis of alpha-particle-emitting targeted radiotherapeutics using histological images. J Nucl Med. 2003; 44(5):792–805. [PubMed: 12732682]
63. Akabani G, Zalutsky MR. Microdosimetry of astatine-211 using histological images: Application to bone marrow. Radiat Res. 1997; 148(6):599–607. [PubMed: 9399706]
64. Chouin N, Bernardeau K, Bardies M, et al. Evidence of extranuclear cell sensitivity to alpha-particle radiation using a microdosimetric model. II. Application of the microdosimetric model to experimental results. Radiat Res. 2009; 171(6):664–673. [PubMed: 19580473]
65. Chouin N, Bernardeau K, Davodeau F, et al. Evidence of extranuclear cell sensitivity to alpha-particle radiation using a microdosimetric model. I. Presentation and validation of a microdosimetric model. Radiat Res. 2009; 171(6):657–663. [PubMed: 19580472]
66. Roeske, JC.; Humm, JL. Microdosimetry of targeted radionuclides. In: Zaidi, H.; Sgouros, G., editors. Therapeutic Applications of Monte Carlo in Nuclear Medicine. Bristol, UK: Institute of Physics Publishing, Ltd; 2003. p. 204-213.
67. Humm JL. Amicrodosimetric model of astatine-211 labeled antibodies for radioimmunotherapy. Int J Radiat Oncol Biol Phys. 1987; 13(11):1767–1773. [PubMed: 3667382]
68. Dewaraja YK, Frey EC, Sgouros G, et al. MIRD pamphlet no, 23: Quantitative SPECT for patient-specific 3-dimensional dosimetry in internal radionuclide therapy. J Nucl Med. 2012; 53(8):1310–1325. [PubMed: 22743252]
69. Dewaraja YK, Ljungberg M, Green AJ, et al. MIRD pamphlet no, 24: Guidelines for quantitative ^{131}I SPECT in dosimetry applications. J Nucl Med. 2013
70. Marcatili S, Pettinato C, Daniels S, et al. Development and validation of RAYDOSE: A Geant4-based application for molecular radiotherapy. Phys Med Biol. 2013; 58(8):2491–2508. [PubMed: 23514870]
71. Botta F, Mairani A, Hobbs RF, et al. Use of the FLUKA Monte Carlo code for 3D patient-specific dosimetry on PET-CT and SPECT-CT images. Phys Med Biol. 2013; 58(22):8099–8120. [PubMed: 24200697]
72. Chiavassa S, Bardies M, Guiraud-Vitaux F, et al. OEDIPE: A personalized dosimetric tool associating voxel-based models with MCNPX. Cancer Biother Radiopharm. 2005; 20(3):325–332. [PubMed: 15989479]

73. Guy MJ, Flux GD, Papavasileiou P, et al. RMDP: A dedicated package for ^{131}I SPECT quantification, registration and patient-specific dosimetry. Cancer Biother Radiopharm. 2003; 18(1):61–69. [PubMed: 12667309]
74. Health NIo. NIH Director's Blog.
75. O'Donoghue JA, Bardies M, Wheldon TE. Relationships between tumor size and curability for uniformly targeted therapy with beta-emitting radionuclides. J Nucl Med. 1995; 36(10):1902–1909. [PubMed: 7562062]
76. Savolainen S, Konijnenberg M, Bardies M, et al. Radiation dosimetry is a necessary ingredient for a perfectly mixed molecular radiotherapy cocktail. Eur J Nucl Med Mol Imaging. 2012; 39(3): 548–549. [PubMed: 22241725]
77. Walrand S, Hanin FX, Pauwels S, et al. Tumour control probability derived from dose distribution in homogeneous and heterogeneous models: Assuming similar pharmacokinetics, (125)Sn-(177)Lu is superior to (90)Y-(177)Lu in peptide receptor radiotherapy. Phys Med Biol. 2012; 57(13):4263–4275. [PubMed: 22705627]
78. Akudugu JM, Howell RW. A method to predict response of cell populations to cocktails of chemotherapeutics and radiopharmaceuticals: Validation with daunomycin, doxorubicin, and the alpha particle emitter-210Po. Nucl Med Biol. 2012; 39(7):954–961. [PubMed: 22503536]

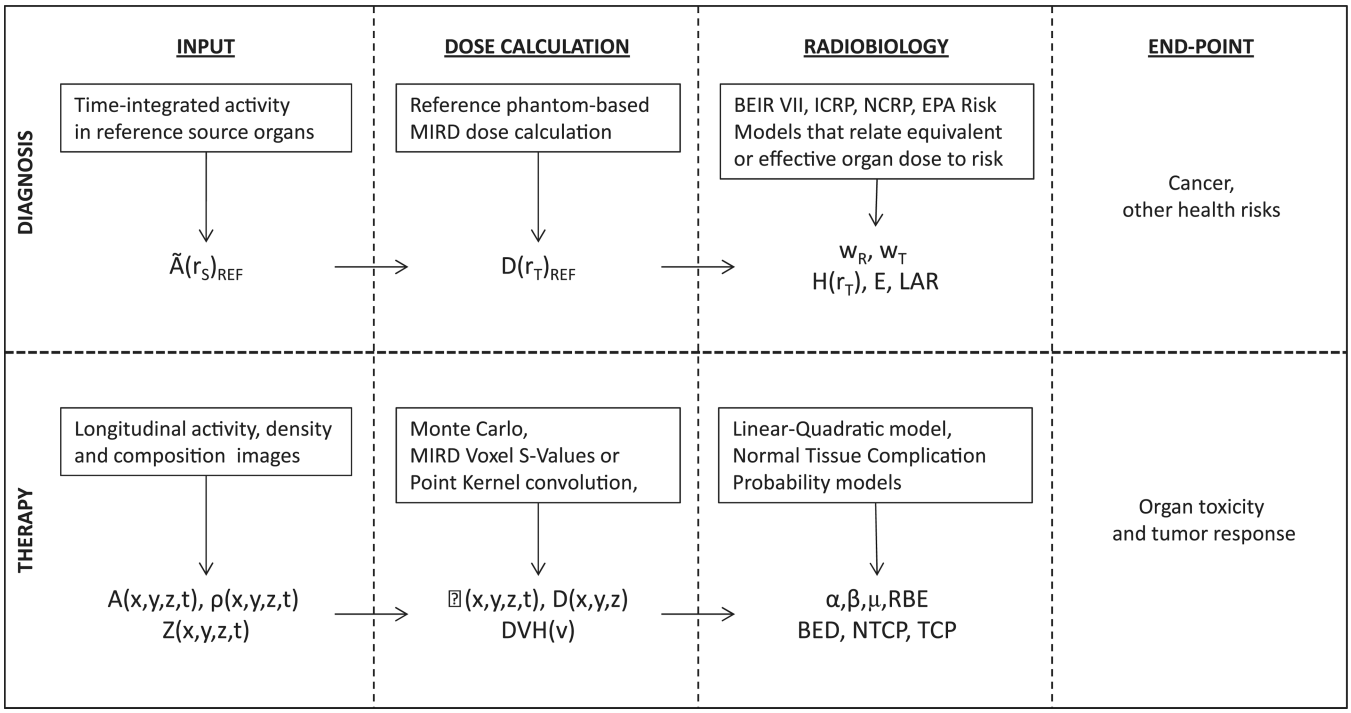

Figure 1.

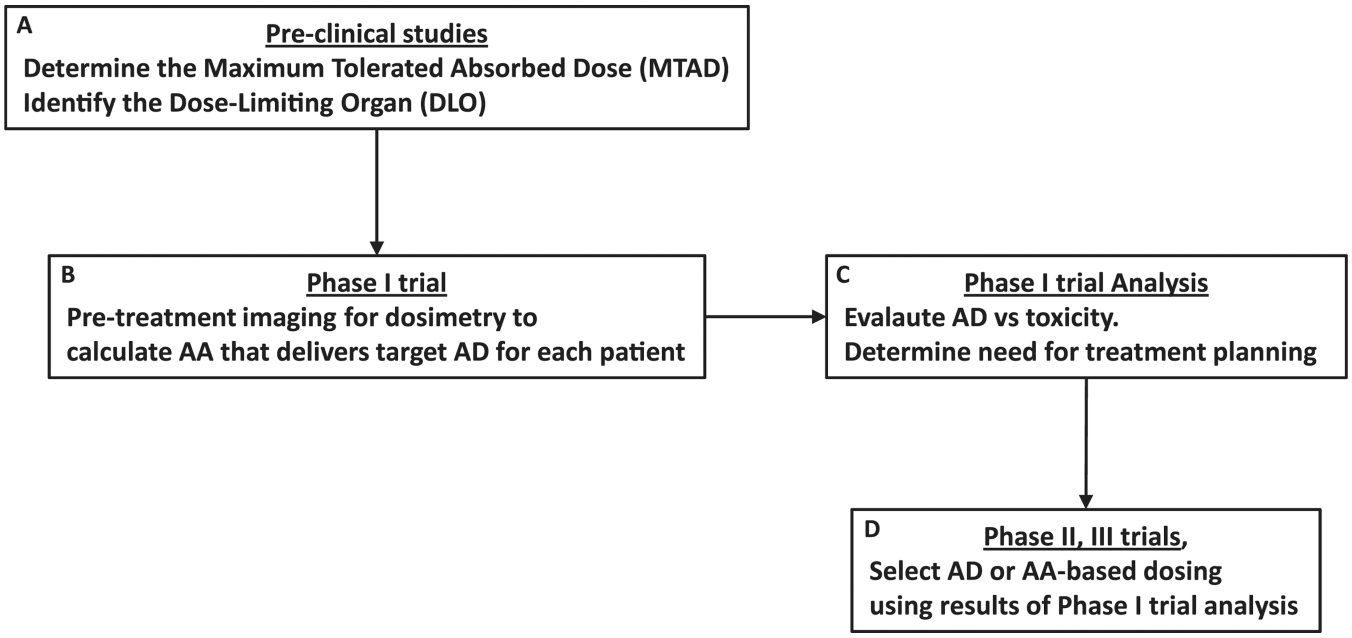

Figure 2.

Table1

Quantity	Description
$\tilde{A}$ (r_S)REF	Time-integrated activity in source region, *S*, of a reference anatomical model
$D(r_T)$REF	Absorbed dose to target region, *T*, of a reference anatomical model
w_R and w_T	Radiation and tissue-weighting factors, respectively
H (r_T), E, and LAR	Equivalent dose to target region, *T*, of a reference model, effective dose to a reference model, and lifetime attributable risk, respectively
$A(x,y,z,t)$, $\rho(x,y,z,t)$, and $Z(x,y,z,t)$	Spatiotemporal map of the activity, tissue density, and tissue composition (atomic number [*Z*]-value), respectively
(x,y,z,t), $D(x,y,z)$, and DVH(ν)	Absorbed dose-rate, absorbed dose, and dose-volume histogram for a patient-specific tissue volume, v, respectively
α and β	Tissue-specificcoefficients of radiation damage proportional to dose (single event is lethal) and dose squared (2 sublethal events required for lethal damage), respectively
μ and RBE	DNA repair rate assuming exponential repair of DNA damage, relative biological efficacy
BED, NTCP, and TCP	Biological effective dose, normal tissue complication probability, and tumor control probability, respectively